

The primordial origin of Jupiter mass Binary Objects

Leiden Observatory, University of Leiden, Niels Bohrweg 2, 2333 CA Leiden
e-mail: hochart@mail.strw.leidenuniv.nl e-mail: spzstrw.leidenuniv.nl

Received XXXXX; accepted XXXXXX

ABSTRACT

Aims.

Methods.

Results.

Key words. gravitational waves – stars: black holes – galaxies: nuclei – stars: kinematics and dynamics – black hole physics

1. Introduction

Recently Pearson & McCaughrean (2023) reported on the discovery of 42 jupiter-mass binaries in the direction of the Trapezium cluster. Their component masses are between $0.6 M_{\text{Jup}}$ and $14 M_{\text{Jup}}$ with projected separations between 25 au and 380 au. Two of these objects have a nearby tertiary jupiter-mass companion, and they found an additional population of 540 single objects in the same mass range. This discovery initiates the discussions on their origin and surviveability in a clustered environment.

Jupiter-mass free floaters have been found before, but they are generally isolated or with small (few au) separations (Kirkpatrick et al. 2021). Known interstellar jupiter-mass binary objects include

- 2MASS J11193254-1137466 AB: a 5 to $10 M_{\text{Jup}}$ primary in a $a = 3.6 \pm 0.9$ au orbit (Best et al. 2017).
- WISE 1828+2650: a 3 to $6 M_{\text{Jup}}$ primary with a $5 M_{\text{Jup}}$ companion in an $\gtrsim 0.5$ au orbit (Beichman et al. 2013).
- WISE J0336-014: a 8.5 to $18 M_{\text{Jup}}$ primary with a 5 to $11.5 M_{\text{Jup}}$ companion in a $0.9^{+0.05}_{-0.09}$ au orbit (Calissendorff et al. 2023).
- 2MASS J0013-1143 discovered by Kellogg et al. (2017) and suspected to be a binary by Eriksson et al. (2019).

Star formation, from the collapse of a molecular cloud through gravitational instability, generally is expected to lead to objects considerably more massive than Jupiter (Low & Lynden-Bell 1976; Boyd & Whitworth 2005). As a consequence, the large population of jupiter-mass free-floaters is considered to result from the ejected planets from dynamically unstable planetary systems. Several studies considered the possibility of planetary systems losing outer-planets in dynamical interactions in dense stellar systems (see i.e., (Rasio & Ford 1996; Zheng et al. 2015; Cai et al. 2017; Flammini Dotti et al. 2019; van Elteren et al. 2019)), but they focus on the ejection of single planets, not binaries. Their origin through dynamical phenomena is further complicated by the tendency for lower mass planets to be more prone to ejections (Ford et al. 2001; Hao et al. 2013; Flammini Dotti et al. 2019; Stock et al. 2020).

We naively recognize four main scenarios for producing JuMBOs. Alternative to forming in situ (which we call scenario *ISF*), one can naively imagine three mechanisms to form

jupiter mass binary objects (JuMBOs) (Wang et al. 2023) argued that these binaries could be explained from planetary systems of which the outer two planets are stripped by a passing star in a close encounter. The two ejected planets would lead to a population of free floating planets, but could also explain the observed population of JuMBOs. We call this scenario *SPF*.

Alternatively one could imagine JuMBOs to result from planet-moon pairs orbiting some star that is ejected to become a jumbo. We call this scenario *SPM*.

Finally, one could imagine that with a sufficiently large population of free-floating jupiter-mass objects could lead to a population of jumbos by dynamical capture of one jupiter by another. We call this scenario *FFC*. A similar scenario was proposed by Kouwenhoven et al. (2010) for explaining very wide stellar pairs, but the model was also adopted to account for wide planetary orbits (Perets & Kouwenhoven 2012).

We start by discussing some fundamental properties of the environmental dynamics, followed by a description of numerical simulations to characterize the parameters of the acquired jumbos and the resulting occurrence rates.

2. The dynamical characterization of JuMBOs

The JuMBOs discovered by Pearson & McCaughrean (2023) were located in the Trapezium cluster. Assessing the cluster dynamics we base our analysis on the analysis carried out by Portegies Zwart (2016). He determined cluster parameters by numerical modeling of the distribution of disk sizes observed in the Trapezium cluster, and concluded that this distribution is best reproduced for a cluster containing some 2500 stars with a total mass of $\sim 880 M_{\odot}$ and a half-mass radius of ~ 0.5 pc. The results were only consistent with the observations if the initial cluster density distribution represented a fractal dimension of 1.6, and was inconsistent with a Plummer (1911) distribution. For consistency with earlier studies, we perform our analysis for Plummer as well as for a fractal (with fractal dimension 1.6) distributions.

Adopting a Plummer distribution of the Trapezium cluster (with a $r_{\text{vir}} = 0.5$ pc virial radius) would have a core radius of $r_c \simeq 0.64 r_{\text{vir}} \sim 0.32$ pc with a core mass of $250 M_{\odot}$, which results in a velocity dispersion of $v_{\text{disp}} \equiv GM/(r \sqrt{r_c^2 + r_{\text{vir}}^2}) \simeq 0.97$ km/s. With a mean stellar mass in the cluster core of $1 M_{\odot}$

the unit of energy expressed in the kinematic temperature kT becomes $\sim 8 \cdot 10^{42}$ erg.

Jumbos are found in the mass range of about $0.6 M_{\text{Jup}}$ to $14 M_{\text{Jup}}$ and with a projected separation of 25 au and ~ 380 au. The averaged observed values are $d = 200 \pm 109$ au, $\langle M \rangle = 4.73 \pm 3.48 M_{\text{Jup}}$, and $\langle m \rangle = 2.81 \pm 2.29 M_{\text{Jup}}$. For clarity we adopt here that the observed range in projected distances between the two jupiter-mass objects is consistent with an orbital separation, and express distances in terms of semi-major axis instead.

To first order, the binding energy of jumbos then ranges between $\sim 5 \cdot 10^{37}$ erg and $1.4 \cdot 10^{41}$ erg, or at most ~ 0.02 kT. Which makes them soft upon an encounter with a cluster star.

The hardest JuMBO, composed of two $14 M_{\text{Jup}}$ planets in a 25 au orbit would be hard for another encountering object of less than $17 M_{\text{Jupiter}}$. For an encountering $1 M_{\text{Jup}}$ object a 25 au orbit would be hard only if the two planets are about three times as massive a Jupiter. The majority of jumbos in the trapezium cluster are then still soft for any encountering free floating planet, but hard if their orbits are tighter, or the encountering free floating planet has low mass.

On average, soft encounters tend to soften these binaries even further (Heggie 1975), although an occasional soft encounter with another planet may actually slightly harden the jumbo. A low impact-parameter encounter with a star will tend to ionize any of the observed jumbos. Independent of how tight the orbit. Jumbos, therefore, are expected to be relatively short lived, and dissociate upon a close encounter with any other cluster member.

To further understand the dynamics of the jumbos in a clustered environment, and to study the efficiency of the various formation scenario's we perform N -body calculations of a Trapezium-like star cluster with a population of jupiter-mass objects in various initial configurations.

3. Model calculations

For each of our proposed models, *ISF* (in situ formation of jumbos), *SPM* (as outer planets orbiting a star), *SPM* (as bound planet-moon pairs orbiting a star), and *FFC* (as mutual capture of free-floaters) we perform a series of N -body simulations with properties consistent with the Trapezium cluster.

Each cluster starts with 2500 single stars taken from a broken power-law mass-function (Kroupa 2002) between $0.08 M_{\odot}$ and $30 M_{\odot}$ distributed either in a Plummer sphere (model Pl) or a fractal distribution with a fractal dimension of 1.6 (model Fr). All models start in virial equilibrium. We run three models for each set of initial conditions, with a virial radius of 0.25 pc, 0.5 pc and 1.0 pc, called model R025, R05 and R100, respectively. We ignore stellar evolution, as well as the tidal field of the Galaxy.

For each of our proposed models, we initialize a population of single or binary jupiter-mass objects. The single (and primaries in primordial jumbos) are selected from a power-law mass function between $0.8 M_{\text{Jup}}$ and $14 M_{\text{Jup}}$, which is consistent with the observed mass function (Pearson & McCaughrean 2023). We fitted a power-law to the primary-planet mass function, which has a slope of $\alpha_{\text{JuMBO}} = -1.2$ (considerably flatter than Salpeter's $\alpha_{\text{Salpeter}} = -2.35$).

For the models with free-floating jupiter-mass objects, scenario *FFC*, we sprinkle the single planets in the cluster potential as single objects using the same initial distribution function as we used for the single stars. These models were run with 1200 jupiter-mass objects (or 600 pairs), but we performed additional runs with 10^3 and 10^4 free floaters.

primordial JuMBOs are initialized with semi-major axis with a flat distribution between 10 au and 10^3 au, an eccentricity from the thermal distribution between 0 and 1, and a mass ratio (also from the thermal distribution) between 0.2 and 1. The binary is subsequently rotated to a random orientation. We typically start with 1200 single or 600 jupiter-mass pairs.

Isolated binaries, for scenario *ISF*, are subsequently sprinkled in the cluster potential as single objects using the same initial distribution function as used for the single stars.

For scenario *SPM* we put the bound planet-moon pair in orbit around a star. The orbit of the planet-moon pair is circular and with a random orientation at a distance from the star such that the planet-moon's orbital separation is one-third of it's Hill radius. This guarantees a stable planet-moon pair in orbit around the selected star.

We selected the star to host such a planet-moon pair from 150 stars lower in mass than $0.6 M_{\odot}$ and 150 more stars. The mid-mass point (of $0.6 M_{\odot}$) is almost twice the mean stellar mass in the mass function.

For scenario *SPP*, we select the same planet masses as for the primordial JuMBOs except that we have them orbiting one of the selected stars as a hierarchical planetary system. The distance from the first planet a_1 and the second planet a_2 (such that $a_2 > a_1$) are selected according to various criteria. The inner orbit a_1 was selected between 20 au and 2000 au from a flat distribution in a . The outer orbit, a_2 , we typically chose to be ten times larger than the inner planet's Hill radius, but we also perform simulations with five times and twice the Hill radius (we call them model rH10, rH05 and rH02, respectively).

We perform an additional series of runs with pre-specified orbital separations for the two planets a_1 and a_2 , to follow the model proposed in Wang et al. (2023).

Each run was repeated 10 times to deal with potential statistical fluctuations, but we run 40 initiations of models *SPP*_Pl_R025.

Each simulation is stopped at an age of 1 Myr, after which we study the population of free floating jupiter-mass objects and the population of JuMBOs.

To summarize, we performed the following model calculations:

<i>SPP</i>	As outer orbiting planets
<i>SPM</i>	As bound planet-moon pair orbiting a star
<i>FFC</i>	Free floating single planets.
<i>ISF</i>	In situ formation of jumbos

4. Results

4.1. Model *SPP*

In scenario *SPP*, we follow the dynamical evolution of 1900 single stars, and 600 stars what are orbited by two planets. According to Wang et al. (2023), jumbos form naturally upon a dynamical encounter between the planetary systems and a passing star. In table 1 we summarize the results of model *PP*.

The *SPP* model calculations fail to reproduce the observed population of JuMBOs. With a total of 600 planetary systems with two jupiter-mass inner orbits between $a_1 = 20$ au and 2000 au the number of JuMBOs is still too low by about a factor 100, and their orbital separations are about an order of magnitude too large. The fractal initial conditions produce even less JuMBOs although the few that formed have considerably smaller orbital separations. Changing the initial distribution in semi-major axis of the inner orbit from a uniform distribution to

Table 1. ...

model	$n_{(s,j)}$	$n_{(j,j)}$	n_j	$\langle M \rangle$	$\langle m \rangle$	$\langle a \rangle$	$\langle e \rangle$
<i>SPP</i> _PI_R025		0.4	0	7.35	2.3	2388	0.70
<i>SPP</i> _PI_R050		0.7	0	6.76	2.44	2196	0.86
<i>SPP</i> _PI_R100		0.4	0	3.77	1.67	1507	0.28
<i>SPP</i> _Fr_R025		0.0	0	—	—	—	—
<i>SPP</i> _Fr_R050		0.1	0	3.8	1.9	118	0.99
<i>SPP</i> _Fr_R100		0.2	0	8.3	5.8	147	0.94

Table 2. ...

model	$n_{(s,j)}$	$n_{(j,j)}$	n_j	$\langle M \rangle$	$\langle m \rangle$	$\langle a \rangle$	$\langle e \rangle$
<i>SPM</i> _PI_R05		286.5	82.3	4.19	3.24	224.9	0.21
<i>SPM</i> _Fr_R05		61.7	113.6	4.90	3.55	175.8	0.47

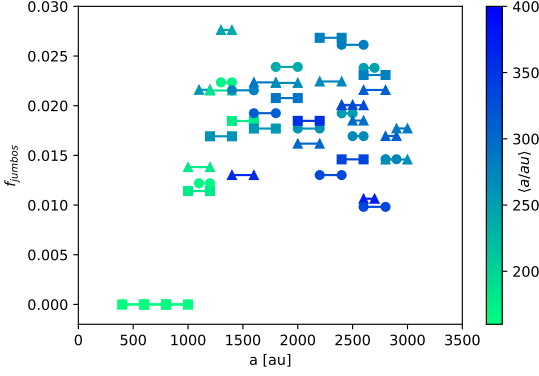


Fig. 1. The number of jumbo's produced in model *SPP*, as fraction of the number of free floating planets for various simulations starting with a Plummer sphere with a virial radius of 0.5 pc. The bullet points along each line correspond with the adopted orbital separation of the two planets (a_1 and a_2). The red symbols indicate an average orbital separations for the jumbos between 25 au and 380 au. The black symbols are outside this regime. The symbol sizes give the number of jumbos (see top right for scaling) in the particular simulation.

a logarithmic distribution reduces the formation rate of JuMBOs even further.

To further explore the failure of model *SPP*, we perform an additional series of simulations with pre-determined inner and outer orbital separations a_1 and a_2 using the Plummer distribution with virial radii of 0.25 pc, 0.50 pc and 1.0 pc for the stars. According to Wang et al. (2023), the eventual orbital separation of the JuMBO would be consistent with the difference in orbital separation between the two planets when orbiting the star. For this reason we perform an additional series of runs with a mutual separation $a_2 - a_1 = 200$ au, expecting those to lead to consistent results in comparison with the observations. The results of these simulations are presented in figure 1.

For these models the JuMBO formation efficiency peaks for an orbital separation $a_1 \gtrsim 800$ au, but steeply drops for smaller values of a_1 . As proposed by Wang et al. (2023), we adopt an difference in the initial orbital distance of about $a_2 - a_1 = 100$ au or 200 au (see figure 1), which would lead to JuMBO orbits in the same range. We performed a total of 45 calculations with various ranges of a_1 and a_2 , of which 39 produced a total of 910 JuMBOs. The initial mean value of $a_1 - a_2 = 167 \pm 38$ au, leading to a final orbital separation of the jumbos of $a_j \sim 262 \pm 45$ au. The claim made by Wang et al. (2023), that the separation distance $a_2 - a_1$ leads to JuMBOs with a similar orbital distance seems reasonable.

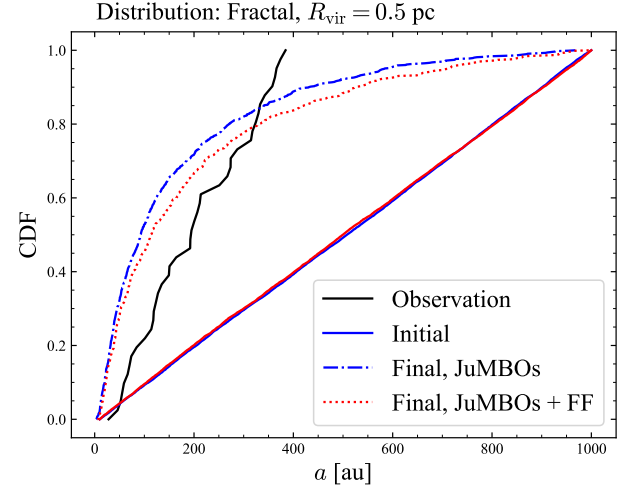


Fig. 2.

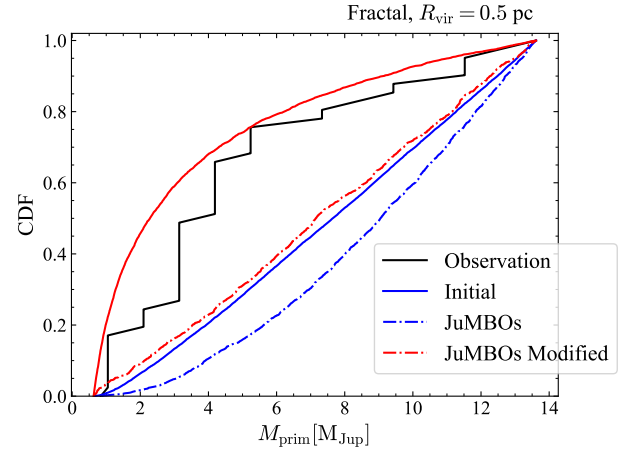


Fig. 3.

4.2. Model *SPM*

4.3. Model *FFC*

4.4. Model *ISF*

4.5. stellar and planetary collisions

We did not find any collisions between stars or planets in a Plummer models, but in the fractal models collisions are rather common.

in the *SPM* models 12.9 ± 8.0 stars experienced a collision with another star. No planets collided with other planets, or with a star.

5. Discussion

They calculate the rate by means of 4-body scattering experiments, in which a star with two equal-mass planets with semi-major axes a_1 for the inner and a_2 for the other planet, encoun-

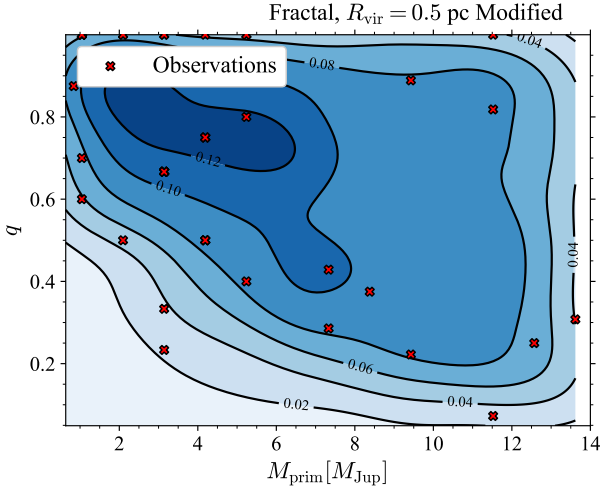


Fig. 4.

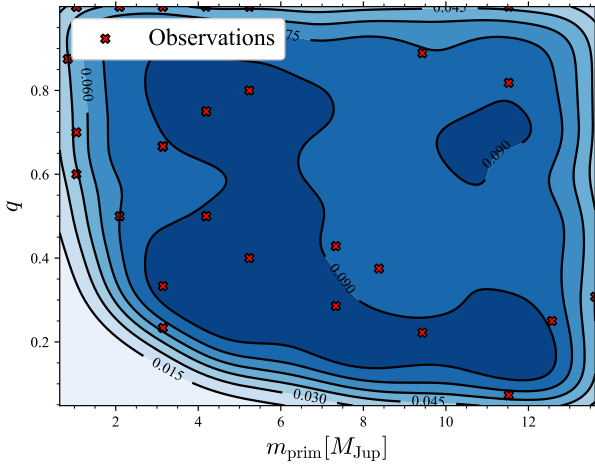


Fig. 5.

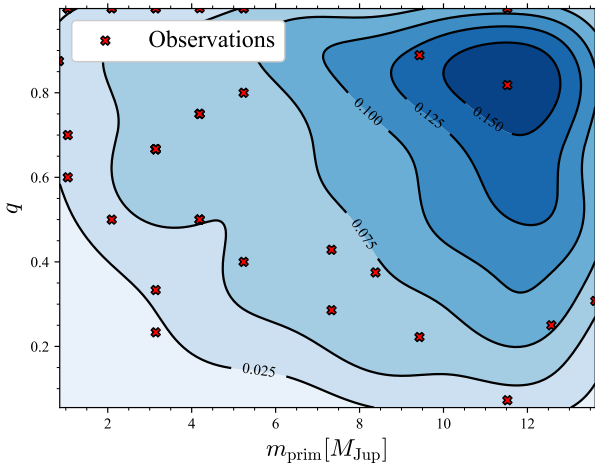


Fig. 6.

ters a single star. Their largest cross section of roughly a_1^2 is obtained if the encounter velocity $0.8v_*/v_1$. For an encounter at the cluster's velocity dispersion, the inner planet would then have a orbital separation of about 900 au around a $1 M_\odot$ star.

The orbital separation of the eventual jumbo would then be comparable to the difference in orbital separation between the two planets ($a_{\text{jumbo}} \simeq a_2 - a_1$).

The model in which JuMBOs form a natural byproduct of the low-mass end of the star-formation process

5.1. The failure of model *SPP*

Note that an inner orbital separation of $a_1 = 800$ au for a $10 M_{\text{Jup}}$ planet leads to a Hill radius of about 150 au. An orbit with $a_2 = 1000$ au, the is probably only marginally stable. Stille, even in those runs the total number of JuMBOs remains small compared to the number of free floaters.

In Wang et al. (2023), the highest cross section is achieved for the orbital velocity of the inner-most planet as fraction of the typical encounter velocity $v_1/v_{\text{disp}} \sim 0.8$. With a cluster velocity dispersion of ~ 0.8 km/s, the orbital velocity roughly 1 km/s. Around a $1 M_\odot$ star such a velocity is obtained, assuming a Kepler orbit, at an orbital separation of 800 au. It turns out, that the results of the cross section calculations performed by Wang et al. (2023) are consistent with our direct N-body simulation, but that the adopted initial orbital separation is too wide in comparison with a realistically population of inner planetary orbits for jupiter-mass planets. Observational selection effect in finding $\gtrsim 800$ au jupiter-mass planets are quite severe, but we consider it unrealistic to have 600 out of 2500 stars to be orbited by such wide planetary systems. In particular, when one considers the small sizes of the observed disks in the Trapezium cluster, which today are all smaller than 400 au (Vicente & Alves 2005).

5.2. JuMBOs as former planet-moon pairs

According to Chen et al. (2023), jumbos form naturally upon a dynamical encounter between two stars one of which with orbited by a binary planet or planet-moon system.

Both calculations Wang et al. (2023) and Chen et al. (2023) adopt scattering experiments to determine the formation rate of jumbos from their adopted initial conditions.

6. Discussion

Chen et al. (2023) argued that JuMBOs potentially originate from tilted circum-binary planets. Formed as a –sort-of– planet-moon system in a wide orbit around a star, that is stripped from the host star by the cluster potential or a relatively wide encounter with another star.

7. Conclusion

Acknowledgements

Veronica Saz Ulibarrena, Shuo Huang, Maite Wilhelm, Brent Maas

References

- Beichman, C., Gelino, C. R., Kirkpatrick, J. D., et al. 2013, ApJ, 764, 101
- Best, W. M. J., Liu, M. C., Dupuy, T. J., & Magnier, E. A. 2017, ApJL, 843, L4
- Boyd, D. F. A. & Whitworth, A. P. 2005, A&A, 430, 1059
- Cai, M. X., Kouwenhoven, M. B. N., Portegies Zwart, S. F., & Spurzem, R. 2017, MNRAS, 470, 4337
- Calissendorff, P., De Furio, M., Meyer, M., et al. 2023, ApJL, 947, L30
- Chen, C., Martin, R. G., Lubow, S. H., & Nixon, C. J. 2023, arXiv e-prints, arXiv:2310.15603
- Eriksson, S. C., Janson, M., & Calissendorff, P. 2019, A&A, 629, A145

- Flammini Dotti, F., Kouwenhoven, M. B. N., Cai, M. X., & Spurzem, R. 2019, *MNRAS* , 489, 2280
- Ford, E. B., Havlickova, M., & Rasio, F. A. 2001, *Icarus* , 150, 303
- Hao, W., Kouwenhoven, M. B. N., & Spurzem, R. 2013, *MNRAS* , 433, 867
- Heggie, D. C. 1975, *MNRAS* , 173, 729
- Kellogg, K., Metchev, S., Miles-Pérez, P. A., & Tannock, M. E. 2017, *AJ* , 154, 112
- Kirkpatrick, J. D., Gelino, C. R., Faherty, J. K., et al. 2021, *ApJS* , 253, 7
- Kouwenhoven, M. B. N., Goodwin, S. P., Parker, R. J., et al. 2010, *MNRAS* , 404, 1835
- Kroupa, P. 2002, *Science*, 295, 82
- Low, C. & Lynden-Bell, D. 1976, *MNRAS* , 176, 367
- Pearson, S. G. & McCaughrean, M. J. 2023, arXiv e-prints, arXiv:2310.01231
- Perets, H. B. & Kouwenhoven, M. B. N. 2012, *ApJ* , 750, 83
- Plummer, H. C. 1911, *MNRAS* , 71, 460
- Portegies Zwart, S. F. 2016, *MNRAS* , 457, 313
- Rasio, F. A. & Ford, E. B. 1996, *Science*, 274, 954
- Stock, K., Cai, M. X., Spurzem, R., Kouwenhoven, M. B. N., & Portegies Zwart, S. 2020, *MNRAS* , 497, 1807
- van Elteren, A., Portegies Zwart, S., Pelupessy, I., Cai, M. X., & McMillan, S. L. W. 2019, *A&A* , 624, A120
- Vicente, S. M. & Alves, J. 2005, *A&A* , 441, 195
- Wang, Y., Perna, R., & Zhu, Z. 2023, arXiv e-prints, arXiv:2310.06016
- Zheng, X., Kouwenhoven, M. B. N., & Wang, L. 2015, *MNRAS* , 453, 2759